Catalytic Activity of the Rh Surface Oxide: CO Oxidation over Rh(111) under Realistic Conditions

ARTICLE *in* THE JOURNAL OF PHYSICAL CHEMISTRY C · FEBRUARY 2010

Impact Factor: 4.77 · DOI: 10.1021/jp910988b

Catalytic Activity of the Rh Surface Oxide: CO Oxidation over Rh(111) under Realistic Conditions

J. Gustafson,*,† R. Westerström,† O. Balmes,‡ A. Resta,‡ R. van Rijn,‡,¶ X. Torrelles,§ C. T. Herbschleb,¶ J. W. M. Frenken,¶ and E. Lundgren†

Division of Synchrotron Radiation Research, Lund University, Box 118, SE-221 00, Sweden, ESRF, 6, rue Jules Horowitz, F-38043 Grenoble cedex, France, Kamerlingh Onnes Laboratory, Leiden University, P.O. Box 9504, 2300 RA Leiden, The Netherlands, and Institut de Ciència de Materials de Barcelona (C.S.I.C), 08193, Bellaterra, Barcelona, Spain

Received: November 19, 2009; Revised Manuscript Received: January 27, 2010

Using a combination of surface X-ray diffraction and mass spectrometry at realistic pressures, the CO oxidation reactivity of a Rh(111) model catalyst has been studied in conjunction with the surface structure. The measurements show that a specific thin surface oxide is always present in the high activity regime of Rh-based CO oxidation.

Introduction

Transition metal-based catalysts form the basis of much of modern chemistry. The catalysis related properties of these metals have therefore been extensively explored under ultrahigh vacuum (UHV) conditions, using model single-crystal surfaces.[1,2] Especially the relatively simple, though highly industrially relevant, reaction between O_2 and CO to form CO_2 has received a lot of attention. It has been found that while the oxides are generally inactive, due to low adsorption probability for CO, the metallic surface allows for coadsorption of CO and O, which leads to a catalytically active surface. Consequently it has been generally accepted that the active phase of transition metal-based CO oxidation catalysts is metallic and not an oxide.

Recently, however, it has been realized that there may be major differences in the behavior of catalysts under UHV conditions as compared to more realistic conditions,[2] and major efforts have been made in order to perform surface studies under higher pressures. In this process it has been found that the high reactivity of Ru catalysts under high partial pressures of oxygen can be explained by the formation of a thin oxide film exposing RuO_2 (110) facets.[3–5] Further it has been found that the CO_2 production over Pt, Pd, Rh, and Pt−Rh increases significantly in conjunction with the formation of a thin oxide film,[6–11] indicating that the active phase is an oxide structure. In the case of Rh, the active phase was found to be a trilayer O−Rh−O surface oxide, as shown in Figure 1a, which forms on all surface orientations as well as on nanoparticles.[12–19] Thus these results are expected to be relevant also for industrial catalysis based on oxide-supported nanoparticles.

In parallel, several publications by the group of Goodman[20–24] have presented seemingly contradicting results. They identify a "hyperactive" phase when the conditions become more oxidizing or the temperature rises, but they interpret their data as showing that this highly active phase is metallic. By *metallic* we refer to a surface structure where the metal atoms are not (significantly) misplaced from the positions of the clean crystal, and any adsorbed atoms/molecules are found on the surface and not mixed with the metal atoms.

In this paper we present new results on the CO oxidation over Rh(111). Using a combination of in situ surface X-ray diffraction (SXRD) and mass spectrometry, in a new microflow reactor, we show that the reactivity is significantly higher if and only if a specific ultrathin surface oxide is present on the surface, as compared to the metallic phase, confirming our previous results. We also argue that our results do not disagree with those of Goodman's group.

Experimental Section

The measurements were performed in the new in situ SXRD flow reactor chamber at the surface diffraction beamline ID03[25,26] at the European Synchrotron Radiation Facility (ESRF) in Grenoble, France. The wavelength of the incident X-rays was set to 0.690 Å. The sample was aligned according to the bulk Bragg reflections of the Rh substrates. The coordinates (H,K,L) in reciprocal space refer to a basis $(\mathbf{b}_1,\mathbf{b}_2,\mathbf{b}_3)$ with $\mathbf{b}_1$ and $\mathbf{b}_2$ spanning the surface lattice of the Rh(111) substrate, as shown in Figure 1b, and $\mathbf{b}_3$ being perpendicular to the surface plane. The use of the MAXIPIX 2-dimensional detector[27,28] provides images of a small part of reciprocal space, around the detector position. Hence, by postanalyzing the images we can make sure that there is no bulk Rh oxide when we measure the surface oxide, as in Figure 2, and we can get an estimate of the peak width.

The CO oxidation measurements were performed with a constant flow of premixed O_2 and CO into the reactor and a pressure controller (Bronkhorst) keeping the total pressure in the reactor cell at 500 mbar. To have a desired lower partial pressure of reactants, the gas mixture is diluted with inert Ar and/or He. The CO gas line is specially equipped with a copper trap, which can be heated to 575 K in order to remove Ni carbonyls. Scans in reciprocal space relevant for Ni or NiO were regularly performed to ensure a Ni free surface. The setup gives us full control over the partial pressures as well as the sample temperature, while the surface structure can be followed by SXRD in situ during the reaction.

* To whom correspondence should be addressed. E-mail: johan.gustafson@sljus.lu.se.
† Lund University.
‡ ESRF.
¶ Leiden University.
§ Institut de Ciencia de Materials de Barcelona (C.S.I.C).

10.1021/jp910988b

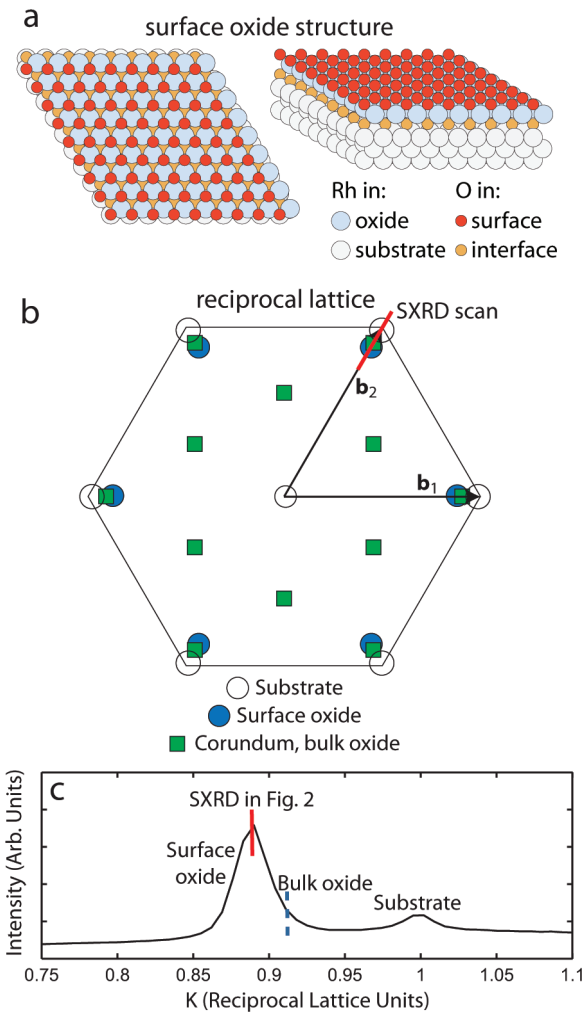

Figure 1. (a) Model of the surface oxide found on all investigated Rh surface orientations, here shown on top of a (111) surface. (b) Map of the reciprocal space corresponding to Rh(111), including the surface oxide and the corundum structured bulk oxide. $\mathbf{b}_1$ and $\mathbf{b}_2$ define the basis in which reciprocal vectors are expressed. The red line shows the direction of the SXRD scan shown in panel c. (c) SXRD scan along the red line in panel b, for a surface oxide covered Rh(111) crystal. The blue (dashed) line marks the position of a reflection from bulk Rh_2O_3, showing that this scan can distinguish between the metallic surface, the surface oxide, and the bulk oxide. During CO oxidation experiments, we have never found the presence of the bulk oxide. Therefore, in the experiments reported below, we only follow the SXRD intensity in the point marked with the red (solid) line in panel c, monitoring whether the surface is in a metallic or surface oxide phase.

In all experiments reported here, the CO partial pressure flowing into the reactor was kept at 7 mbar, while the O_2 partial pressure was varied for different experiments. During all our experiments on CO oxidation over pure Rh we have never seen any signal from Rh bulk oxide. Therefore, in the measurements shown here, we only monitor the intensity from the surface oxide reflection, as indicated in Figure 1c. In this way we may probe whether the surface is in a metallic or surface oxide phase.

The crystal was cleaned as in ref 13. The sample temperature was measured with use of a tungsten−rhenium thermocouple (type C), mechanically clamped between the ceramic heating plate and the sample clips. Also here Ni was avoided in order to eliminate the risk of Ni carbonyl contamination.

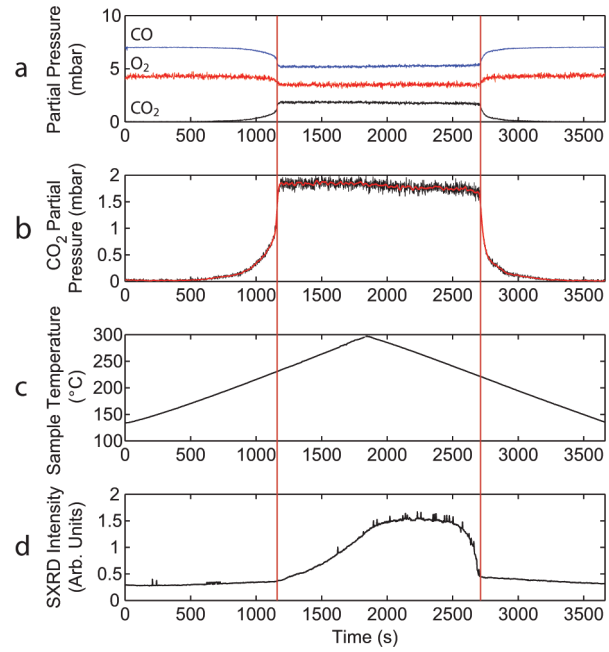

Figure 2. CO oxidation over Rh(111) in a flow of 5 mbar O_2 and 7 mbar CO, while varying the temperature between 140 and 300 °C: (a) Partial pressure of O_2, CO, and CO_2. (b) Zoom-in of the CO_2 partial pressure directly monitoring the catalytic activity. The red line shows smoothened data that are used for further analysis as in Figure 3. (c) Sample temperature. (d) SXRD signal in the surface oxide reflection marked red in Figure 1b.

Results

Figure 2 shows the results of an experiment where a flow of 7 mbar of CO and 5 mbar of O_2 passes the Rh(111) surface, while the sample temperature is varied from 140 to 300 °C and down again. Panel a shows the partial pressures of CO, O_2, and CO_2, panel b is a zoom-in of the CO_2 partial pressure, which directly monitors the catalytic activity, panel c monitors the sample temperature, and panel d shows the SXRD signal in the surface oxide spot marked red in Figure 1, hence monitoring whether the surface is in a metallic or a surface oxide phase.

At the start of the experiment, the CO oxidation activity (Figure 2b) is below the detection limit, due to the low temperature and the surface being poisoned presumably by adsorbed CO.[24] As the temperature increases, the activity follows smoothly until 1200 s, yielding a temperature of 230 °C. Here the activity suddenly rises steeply to a constant upper limit. This is the so-called mass transfer limit (MTL), where the CO_2 production is limited by the amount of reactants that reach the surface rather than by the actual reactivity of the model catalyst. The system stays in the MTL regime until we have cooled the sample to about 220 °C. At this temperature the CO_2 production suddenly decreases and continues to decrease smoothly.

Also the SXRD shows no intensity at the start of the experiment, but after 1200 s the signal increases, verifying the appearance of the surface oxide. When the temperature has reached 300 °C, the oxide signal is at its maximum, and while cooling it disappears rather suddenly between 250 and 220 °C. Note that the points where the surface oxide starts to grow and where it finally disappears perfectly coincide with the switches to and from the MTL regime. *If, and only if, the surface oxide is present, the catalytic activity reaches the MTL.* The low SXRD signal just after the appearance of the surface oxide most likely reflects that oxidation at such low temperatures leads to an oxide structure that is divided into small domains. This

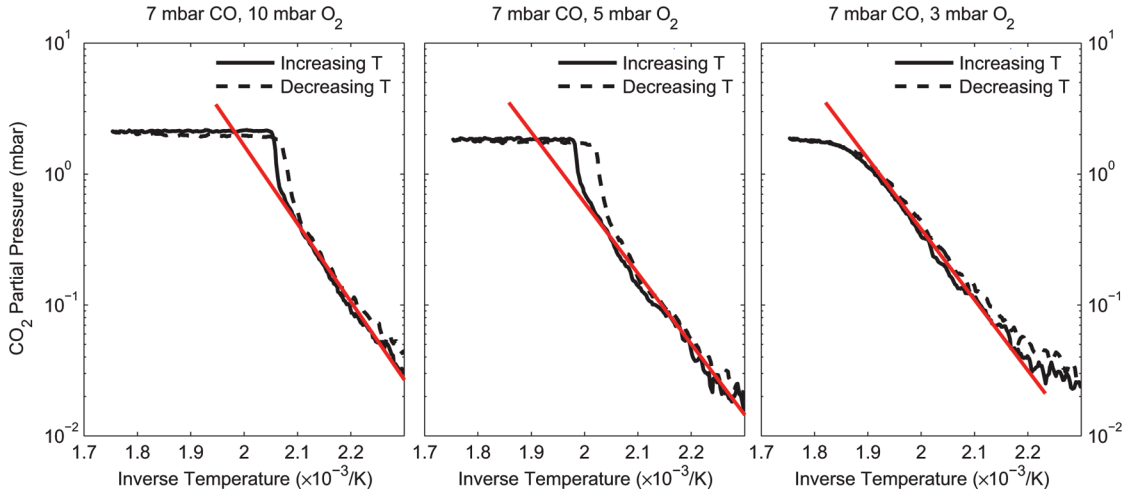

Figure 3. Data from experiments similar to the one shown in Figure 2, with different O_2 partial pressures, presented as Arrhenius plots. The red lines mark the linear behavior of the metallic phase in the absence of the mass transfer limit.

interpretation is supported by the broad peak shape as seen in the 2-dimensional detector (not shown). This is expected since in order to form a nicely ordered surface oxide structure, we need a temperature of at least 400 °C. On the other hand, the low intensity could also indicate that the surface is not completely covered by the surface oxide, and we cannot rule out that there is a coexistence between the surface oxide and metallic patches on the surface. The asymmetry of the SXRD data shows that once a well-ordered surface oxide is formed, it stays well ordered although the temperature drops.

To investigate the difference in reactivity with and without the surface oxide, Figure 3 shows the data from experiments as described above, with three different O_2 partial pressures, plotted as Arrhenius plots. At low temperatures the CO_2 production, in all three cases, follows a linear behavior as expected, with an activation barrier of about 1.1 eV. This is in good agreement with values reported for the activation barrier on a CO dominated metallic surface.[24] When increasing the temperature, we find a sudden step-like increase of the reactivity into the MTL for the cases with O_2 partial pressures of 5 and 10 mbar, i.e., under net oxidizing conditions. As shown in Figure 2, this increase coincides with the switch from a metallic surface to a surface oxide. Since the activity above the increase is higher than expected for the metallic surface at this temperature (indicated with the red lines in Figure 3) it is clear that the surface oxide phase is more reactive than the CO covered metallic phase. Since we are mass transfer limited, however, we cannot deduce how much more reactive the oxide phase is. With 3 mbar of O_2, i.e., slightly net reducing conditions, the step-like increase is absent and the transition into the MTL is smooth. In the corresponding SXRD data (not shown) we also do not see the formation of the surface oxide.

In summary our results show that, under net oxidizing conditions and at high enough temperatures, the Rh surface changes from a metallic phase to a more reactive surface oxide. Imediately after the switch, the SXRD surface oxide signal is weak, which indicates that the surface oxide domains are small. Alternatively there is a coexistence between surface oxide and metallic patches. Under net reducing conditions, the surface phase never changes.

Discussion

We have previously reported results showing that the Rh surface oxide appears in conjunction with a sudden increase of the CO oxidation activity.[10,11] From these results, we concluded that the surface oxide plays a crucial role in the high activity of Rh-based CO oxidation catalysts. Furthermore, since the same surface oxide is formed on all Rh surface orientations, as well as on nanoparticles, these results are expected to be relevant also for industrial catalysts.

On the other hand, recently published results could be interpreted as contradicting our findings.[20,22,24] A highly active phase was identified when either the conditions become more oxidizing or the temperature rises. From in situ PM-IRAS measurements it was found that, during the high activity, there is no signal corresponding to CO adsorbed on an oxide surface. It was also found that the activity peaks exactly in the transition, at which the MTL is reached. Below we present an interpretation implying that these data do not disagree with our results.

As has been noted previously,[9,24,29] the bulk Rh oxide is inactive since CO cannot adsorb on its surface. The same holds for the perfect surface oxide for the same reason.[30] In the high activity regime, however, our measurements clearly show that the surface oxide is present. Furthermore, we have shown previously that the surface oxide can be reduced by CO, even under UHV conditions, and after some activation time, during which the number of active sites is increased, this process is very rapid.[31] Our interpretation of this is that, during the reaction, CO adsorbs either on defects in the surface oxide structure or on the edge of surface oxide islands. CO adsorbed in such sites would not yield the same vibrational signal as CO adsorbed on a well-ordered oxide surface. Furthermore, in ref 31, the reaction is so fast that the amount of adsorbed CO is below the detection limit until the surface is completely reduced. Thus, our interpretation does not disagree with the absence of a PM-IRAS signal corresponding to CO adsorbed on an oxide.

In our measurements we do not find a peak corresponding to an extra active transient phase. We note, however, that the design of the reactor may affect the CO_2 production. With a highly reactive sample, there will be a depletion of reactants near the surface. In the MTL, the depletion is total for the least abundant reactant (CO in the cases where the transient peak is seen[20,22,24]). With a slightly lower reactivity, however, the CO partial pressure at the surface is significantly higher. As a result, if the phase changes abrubtly, as it clearly does in Figure 2, there will be more CO present at the surface during the switch, before the depletion has settled. A higher activity will therefore be measured during the transition than after the transition. This

effect will be larger in a larger batch reactor than in a small flow reactor.

Conclusions

We have studied the relation between surface structure and CO oxidation activity over Rh(111) in realistic flows of O_2 and CO, using a combination of in situ SXRD and mass spectrometry. When heated under net oxidizing conditions, the model catalyst switches to a high activity regime, and when cooled again, it switches back. These switches coincide perfectly with the appearance of a surface oxide signal in the SXRD measurements showing that if and only if the surface oxide is present, the model catalyst is found in the high activity mode. Under net reducing conditions we do not find a similar switch, and the activity follows the behavior expected for a CO-covered metallic surface.

CO does not adsorb easily on either the bulk Rh oxide or the perfect surface oxide, implying that these phases are inactive for CO oxidation. We therefore propose that the surface oxide present during these measurements is rich in defects and/or coexisting with patches of metallic surface, allowing for CO adsorption.

Acknowledgement. .

This work was financially supported by the Swedish Research Council, the Crafoord Foundation, the Anna and Edwin Berger foundation, and the Knut and Alice Wallenberg Foundation. Support by the ESRF staff is gratefully acknowledged. X.T. thanks the Spanish MICINN agency for partially funding this project through project nos. CSD2007-00041 and MAT2009-09308.

References and Notes

(1) Somorjai, G. A. *Introduction to Surface Chemistry and Catalysis*; Wiley: New York, 1994.

(2) *Handbook of Heterogeneous Catalysis*; Ertl, G., Knözinger, H., Schüth, F., Weitkamp, J., Eds.; Wiley-VCH: Weinheim, Germany, 2008.

(3) Over, H.; Kim, Y. D.; Seitsonen, A. P.; Wendt, S.; Lundgren, E.; Schmid, M.; Varga, P.; Morgante, A.; Ertl, G. *Science* **2000**, *287*, 1474–1476.

(4) Over, H.; Mühler, M. *Prog. Surf. Sci.* **2003**, *72*, 3–17.

(5) Over, H.; Balmes, O.; Lundgren, E. *Catal. Today* **2009**, *145*, 236.

(6) Hendriksen, B. L. M.; Frenken, J. W. M. *Phys. Rev. Lett.* **2002**, *89*, 046101-1.

(7) Hendriksen, B. L. M.; Bobaru, S. C.; Frenken, J. W. M. *Surf. Sci.* **2004**, *552*, 229–242.

(8) Ackermann, M. D.; Pedersen, T. M.; Hendriksen, B. L. M.; Robach, O.; Bobaru, S. C.; Popa, I.; Quirós, C.; Kim, H.; Hammer, B.; Ferrer, S.; Frenken, J. W. M. *Phys. Rev. Lett.* **2005**, *95*, 255505-1.

(9) Westerström, R.; Wang, J. G.; Ackermann, M.; Gustafson, J.; Resta, A.; Mikkelsen, A.; Andersen, J. N.; Lundgren, E.; Balmes, O.; Torrelles, X.; Frenken, J. W. M.; Hammer, B. *J. Phys.: Condens. Matter* **2008**, *20*, 184019.

(10) Gustafson, J.; Westerström, R.; Mikkelsen, A.; Torrelles, X.; Balmes, O.; Bovet, N.; Andersen, J. N.; Baddeley, C. J.; Lundgren, E. *Phys. Rev. B* **2008**, *78*, 045423.

(11) Gustafson, J.; Westerström, R.; Resta, A.; Mikkelsen, A.; Andersen, J. N.; Balmes, O.; Torrelles, X.; Schmid, M.; Varga, P.; Hammer, B.; Kresse, G.; Baddeley, C. J.; Lundgren, E. *Catal. Today* **2009**, *145*, 227.

(12) Gustafson, J.; Mikkelsen, A.; Borg, M.; Lundgren, E.; Köhler, L.; Kresse, G.; Schmid, M.; Varga, P.; Yuhara, J.; Torrelles, X.; Quirós, C.; Andersen, J. N. *Phys. Rev. Lett.* **2004**, *92*, 126102.

(13) Gustafson, J.; Mikkelsen, A.; Borg, M.; Andersen, J. N.; Lundgren, E.; Klein, C.; Hofer, W.; Schmid, M.; Varga, P.; Köhler, L.; Kresse, G.; Kasper, N.; Stierle, A.; Dosch, H. *Phys. Rev., B* **2005**, *71*, 115442-1.

(14) Gustafson, J.; Resta, A.; Mikkelsen, A.; Westerström, R.; Andersen, J. N.; Lundgren, E.; Weissenrieder, J.; Schmid, M.; Varga, P.; Kasper, N.; Torrelles, X.; Ferrer, S.; Mittendorfer, F.; Kresse, G. *Phys. Rev., B* **2006**, *74*, 35401-1.

(15) Dri, C.; Africh, C.; Esch, F.; Comelli, G.; Dubay, O.; Köhler, L.; Mittendorfer, F.; Kresse, G.; Dudin, P.; Kiskinova, M. *J. Chem. Phys.* **2006**, *125*, 94701-1.

(16) Klikovits, J.; Schmid, M.; Merte, L. R.; Varga, P.; Westerström, R.; Resta, A.; Andersen, J. N.; Gustafson, J.; Mikkelsen, A.; Lundgren, E.; Mittendorfer, F.; Kresse, G. *Phys. Rev. Lett.* **2008**, *101*, 266104.

(17) Mittendorfer, F.; Seriani, N.; Dubay, O.; Kresse, G. *Phys. Rev. B* **2007**, *76*, 233413.

(18) Nolte, P.; Stierle, A.; Jin-Phillipp, N. Y.; Kasper, N.; Schulli, T. U.; Dosch, H. *Science* **2008**, *321*, 1654.

(19) Jin-Phillipp, N. Y.; Nolte, P.; Stierle, A.; Dosch, H. *Surf. Sci.* **2009**, *603*, 2551.

(20) Chen, M. S.; Cai, Y.; Yan, Z.; Gath, K. K.; Axnanda, S.; Goodman, D. W. *Surf. Sci.* **2007**, *601*, 5326.

(21) Gao, F.; McClure, S. M.; Cai, Y.; Gath, K. K.; Wang, Y.; Chen, M. S.; Guo, Q. L.; Goodman, D. W. *Surf. Sci.* **2009**, *603*, 65.

(22) McClure, S. M.; Goodman, D. W. *Chem. Phys. Lett.* **2009**, *469*, 1.

(23) Gao, F.; Wang, Y.; Cai, Y.; Goodman, D. W. *J. Phys. Chem. C* **2009**, *113*, 174.

(24) Gao, F.; Cai, Y.; Gath, K. K.; Wang, Y.; Chen, M. S.; Guo, Q. L.; Goodman, D. W. *J. Phys. Chem. C* **2009**, *113*, 182.

(25) Balmes, O.; van Rijn, R.; Wermeille, D.; Resta, A.; Petit, L.; Isern, H.; Dufrane, T.; Felici, R. *Catal. Today* **2009**, *145*, 220.

(26) van Rijn, R.; Ackermann, M.; Balmes, O.; Dufrane, T.; Geluk, A.; Gonzalez, H.; Isern, H.; de Kuyper, E.; Petit, L.; Sole, V.; Wermeille, D.; Felici, R.; Frenken, J. *Rev. Sci. Instrum.* **2010**, *81*, 014101.

(27) Llopart, X.; Campbell, M.; Dinapoli, R.; Segundo, D.; Pemigotti, E. *IEEE Trans. Nucl. Sci.* **2002**, *49*, 2279–2283.

(28) Ponchut, C.; Clement, J.; Rigal, J.-M.; Papillon, E.; Vallerga, J.; LaMarra, D.; Mikulec, B. *Nucl. Instrum. Methods Phys. Res., Sect. A* **2007**, *576*, 109–112.

(29) Flege, J. I.; Sutter, P. *Phys. Rev. B* **2008**, *78*, 153402.

(30) Lundgren, E.; Mikkelsen, A.; Andersen, J. N.; Kresse, G.; Schmid, M.; Varga, P. *J. Phys., Condens. Matter* **2006**, *18*, R481–R499.

(31) Lundgren, E.; Gustafson, J.; Resta, A.; Weissenrieder, J.; Mikkelsen, A.; Andersen, J. N.; Köhler, L.; Kresse, G.; Klikovits, J.; Biederman, A.; Schmid, M.; Varga, P. *J. Electron Spectrosc. Relat. Phenom.* **2005**, *144–147*, 367–372.

JP910988B